

# Physical Properties of Engineered Nanocomposites for Defense Applications

Alex Henson, Brendan Evans and Prof. Sanju Gupta (Mentor)

Department of Physics & Astronomy, Western Kentucky University

Bowling Green, KY 42101



**Abstract Synopsis** Polymer nanocomposites are significant for modern and future technologies (aerospace, defense, water purification etc.) due to their tailored properties, lightweight and low cost. However, 'forward' engineered polymer (host matrix) composites with smaller size nanoparticles (guest) providing desired properties targeting specific applications remains a challenging task as they depend largely on nanoparticles size, shape and loading (volume fraction). This study develops polymer nanocomposites impregnated with 'organic-inorganic' silsesquioxane nanoparticles and graphene nanoribbons, and investigates microscopic structure and dynamics of interfacial layer to predict macroscale properties. The nanocomposites consist of poly(2-vinylpyridine) (P2VP) polymer (segment ~ 5nm) with spherical silsesquioxane nanoparticles (diameter ~2-5 nm) and planar nitrogenated graphene nanoribbons (lateral dimension ~5-10 nm), both with attractive (hydrogen bonding and electrostatic) interactions. This approach reinforces the role of molecular parameters controlling the structure and dynamics of interfacial layer in predicting properties. The transmission electron microscopy will reveal microscopic structure and the lattice bonding, interfacial stress transfer and conjugation length are determined from micro-Raman spectroscopy. The glass transition temperature,  $T_g$ , obtained using differential scanning calorimetry reveals positive shift in  $T_g$  values with nanoparticles loadings. We used temperature dependent broadband dielectric spectroscopy to gain fundamental insights into the interfacial layer and diffusion dynamics above and below  $T_g$  and to establish quantitative microstructure-property correlations. <sup>\$\$\$</sup>KY NSF EPSCoR REG and KY NASA UF funding are acknowledged.

**Background and Motivation** Organic and inorganic nanoparticle reinforcements have garnered widespread attention for polymer nanocomposites to yield properties enhancement useful for wide ranging modern technologies including photovoltaics, catalysis, optics, and renewable energy. Recent experiments and computational simulations revealed the macroscale properties are governed by mesoscale structure and interfacial layer dynamics due to the interactions between the polymer matrix (host) and nanoparticle reinforcements (guest). However, a clear fundamental understanding of the role of size, shape, loading (volume fraction) in controlling the structure and dynamics of polymer-nanoparticle interfacial layer is limited. Moreover, 'forward' engineered polymer-nanoparticle composites targeting specific applications often require higher volumetric density and better dispersions remains a challenging task. We report on developing polymer nanocomposites engineered to minimize dielectric losses and investigating structure and dynamics of interfacial layer to predict macroscale properties.

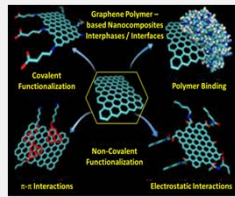


**Figure 1.** Schematic of the blending of graphene-related materials with polymer matrix, covalent versus non-covalent functionalization and electrostatic versus  $\pi-\pi$  interactions at the interfaces.

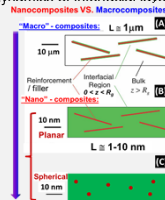


**Figure 2a.** Schematic of polymer-based macrocomposites and nanocomposites with (A) microscale fibers (B) cylindrical nanotubes or planar graphene nanoribbons and (C) spherical nanoparticles along with associated characteristics ( $l$ ,  $z$  and  $R_p$ ) of two-phase interfacial layer model. The smaller nanoparticles cites change in volume of interfacial region for nanocomposites.

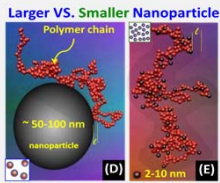


**Figure 2b.** (D) Larger nanoparticles vs. (E) smaller nanoparticles sticking to polymer chain segments producing slower (plastic) or faster (viscoelastic) nanocomposites [7, 9, 31]. The nanoparticles force sites are rendered as spheres and (insets) change in volume of interfacial region is also shown from micro- to nanoscale composites.

**Approach** We prepared a series of solution cast P2VP-based nanocomposites with (1) Graphene Nanoribbons (GNR), (2) organic/inorganic N-POSS caged molecule and (3) graphene oxide (GO) with various concentrations.

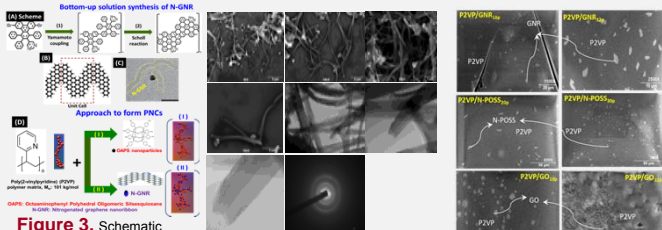
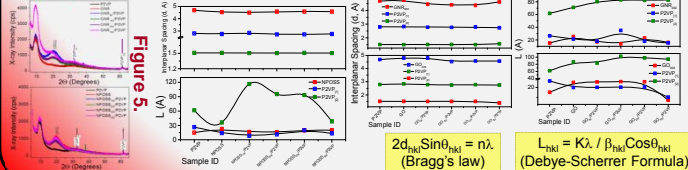


**Figure 3.** Schematic representations of the synthesis employed to prepare 'hybrid' graphene-polymer nanocomposites.

**Figure 4.** Shown are the (left) SEM and TEM images of functionalized GNR along with electron diffraction. The average width of GNR is 30-50 nm. (right) the SEM micrographs of nanocomposites showing uniform dispersion/distribution of nanofillers.

**1) X-ray Diffraction (XRD)**



**Results 2) Raman Spectroscopy (RS) 3) Thermal Properties for Stability and Glass transition Temperature ( $T_g$ )**

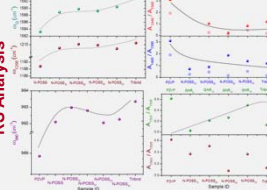
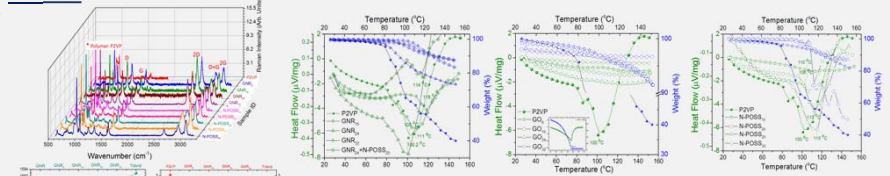


**Figure 6a.** Shown are the Raman spectra reflecting the prominent Raman bands (D, G, and 2D), where G peak is the characteristic for  $sp^2$ -bonded C systems and D band arise due to disorder along with polymer P2VP peaks. The polymer bands are sharp reflective of semicrystalline order.

**Figure 6b.** Shown are Raman spectroscopy maps for the conjugation length ( $\xi$ ) distribution determined by the intensity ratio of prominent bands occurring at 1585  $cm^{-1}$  for GNR, 1200  $cm^{-1}$  for N-POSS and 1440  $cm^{-1}$  for P2VP. The increasing ratio with GNR and N-POSS indicate crystallization enhancement in the vicinity of polymer.

**4) Temperature Dependent Electrical Properties**

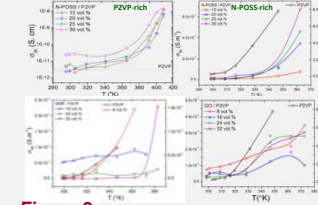


**Figure 9.** Temperature-dependent electrical properties (I-V/T) for all the nanocomposites showing an increase in dc electrical conductivity with temperature (semiconducting or non-linear behavior) and with nanofiller loading.

**Summary** 1. Proposed approaches enabled the desired functional interfaces between polymer and nanofillers enable hydrogen bonding and facilitate interactions, needed for real-world applications. 2. SEM revealed surface morphology showing uniform distribution of nanofillers studied. Likewise, the surface topography measured using AFM determined rms surface roughness and showed uniform distribution. 3. Raman spectroscopy, helps to identify the polymer related and nanofillers bands as well as interfaces. Through quantitative analysis of the prominent Raman bands, we obtained an integral picture of these hybrid nanocomposites and determined microscopic stress and strain for all of the samples studied hereby, which resulted in compressive stress/strain besides increased conjugation length in the vicinity of polymer matrix. 4. Temperature-dependent electrical properties [I-V(T)] displayed apparent semiconducting behavior for all of the nanocomposites. 5. Force spectroscopy technique is used for elasticity mapping of nanocomposites via force-displacement curves, successfully measuring the force constant behavior. These results are unprecedented and quite promising for aerospace, automotive, electronics, photonics, renewable energy sources technologies.

**Figure 7.** Thermo-physical (Differential scanning calorimetry; DSC and Thermogravimetric; TGA) properties of all nanocomposites reflecting a marginal increase in glass transition temperature with increase in loadings, which also indicates increase in thermal stability and thermal conductivity.

**5) Atomic Force Microscopy and Force Spectroscopy for Nanomechanical Properties**

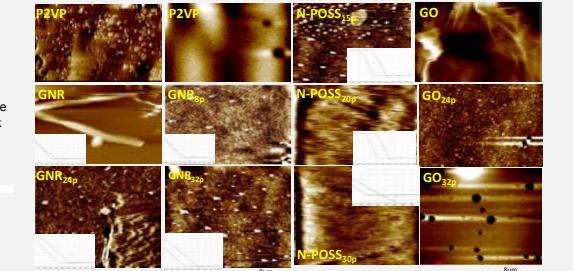


**Figure 8.** Shown are the Force versus Distance (F-x) plots on the topographic surface of polymer nanocomposites namely, GNR/P2VP, N-POSS/P2VP, GO/P2VP along with constituents. The variation in the shape of the retract behavior of the tip is apparent and indicative of both stiff and softer nature of the nanocomposites. These results are unprecedented and provide useful insights into the materials interfaces and interphases.

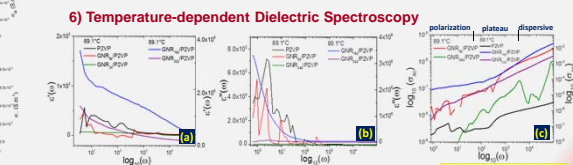
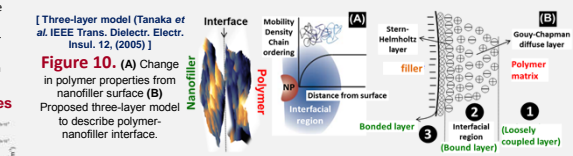


**Figure 11.** Dielectric spectroscopy with temperature for GNR nanocomposites to understand interfacial dynamics.

$$\epsilon''(\omega) = \epsilon''(\omega) - i\epsilon''(\omega)$$

$$\tan \delta = \epsilon''/\epsilon'$$

$$\sigma_{dc} = \epsilon_{dc}^* \omega A d^2$$

(Jonscher's power law)